

CONSTRAINING THE GALACTIC BAR PARAMETERS WITH RED CLUMP GIANTS

Shude Mao^{1,2} [★] and Bohdan Paczyński²

¹ *Univ. of Manchester, Jodrell Bank Observatory, Macclesfield, Cheshire SK11 9DL, UK*

² *Princeton University Observatory, Princeton, NJ 08544-1001, USA*

Accepted . Received ; in original form

ABSTRACT

Red clump giants in the Galactic bulge occupy a distinct region in the colour magnitude diagram. They have a very small spread in intrinsic luminosities and their number counts have a well defined peak. We show that these characteristics can be used to constrain the differences in the streaming motions of stars on the near side and those on the far side. We propose two methods to select two samples with one preferentially on the near side and the other on the far side. In the first method, we divide red clump giants into a bright sample and a faint one; stars in the bright sample will be on average more on the near side and vice versa. The second method relies on the fact that lensed bulge stars lie preferentially on the far side due to the enhanced lensing probability by the stars on the near side and in the disk. If the radial streaming motion is $\approx 50 \text{ km s}^{-1}$, we find the difference in the average radial velocity between the bright and faint samples can reach $\approx 33 \text{ km s}^{-1}$ while the corresponding difference is about $\approx 10 \text{ km s}^{-1}$ between the lensed stars and all observed stars. The difference in the average proper motion between the bright and faint samples is about $\approx 1.6 \text{ mas yr}^{-1}$ if there is a tangential streaming motion of 100 km s^{-1} ; the corresponding shift between the lensed stars and all observed stars is approximately $\approx 1 \text{ mas yr}^{-1}$. To observe the shifts in the radial velocity and proper motion, roughly one hundred microlensing events, and/or bright/faint red clump giants, need to be observed either spectroscopically or astrometrically. The spectroscopic observations can be performed efficiently using multi-object spectrographs already available. The proper motion signature of microlensed objects can be studied using ground-based telescopes

and the Hubble Space Telescope. These observations will provide strong constraints on the Galactic bar parameters.

Key words: gravitational lensing – Galaxy: bulge – Galaxy: centre Galaxy: kinematics and dynamics – Galaxy: structure

1 INTRODUCTION

Many observational groups carried/are carrying out microlensing observations (e.g., MACHO: Alcock et al. 1993; OGLE: Udalski et al. 1993; DUO: Alard & Guibert 1997; MOA: Bond et al. 2001; EROS: Aubourg et al. 1993). Over one thousand microlensing events in the local group have been identified (e.g., Alcock et al. 2000; Woźniak et al. 2001; Derue et al. 2001; Alard & Guibert 1997; Bond et al. 2001). In the coming years, ~ 1000 microlensing events are expected to be discovered by the OGLE III¹ and other collaborations every year, many of them in real-time.

Data collected from microlensing experiments have very diverse applications (for reviews see Paczyński 1996; Gould 1996). One of the most important applications is studying the Galactic structure. There is strong evidence that the centre of Galaxy hosts a bar (e.g., de Vaucouleurs 1964; Blitz & Spergel 1991; Stanek et al. 1994, 1997; Kiraga & Paczyński 1994; Häfner et al. 2000 and references therein). However, the parameters of the bar are not well-determined, including its mass, size, and the motion of stars within it.

Data from microlensing experiments provide several ways of probing the structure of the inner Galaxy. For example, the optical depth is roughly proportional to the total mass of the bar while the event time scale distribution probes the mass function and kinematics of the bar. Another important method that was first explored by Stanek et al. (1997) uses red clump giants (RCGs). These bulge stars occupy a distinct region in the colour-magnitude diagram (see, e.g., Stanek et al. 2000 and references therein). They have very small intrinsic widths in their luminosity function, about 0.2 mag for RCGs in the Galactic bulge (see §2 in Stanek et al. 1997; Paczyński & Stanek 1998). The observed luminosity function has a well-defined peak and an apparent width (see Fig. 5 in Stanek et al. 1997). The apparent width depends on both the intrinsic width and the spread caused by the radial depth of the

* E-mail: smao@jb.man.ac.uk (SM); bp@astro.princeton.edu (BP)

¹ <http://www.astrouw.edu.pl/~ogle/ogle3/ews/ews.html>

bar. Stanek et al. (1997) used this dependence to constrain the Galactic bar axial ratios and orientation.

In this paper, we use the RCGs to study the kinematics of stars in the Galactic bar. Stars on the front side and far side may have different (tangential and radial) streaming motions. We explore two effects to constrain such motions. The first effect is based on the realisation that red clump stars at the bright slope of the peak of the luminosity function must be (on average) closer to us, i.e. on the near (front) side, while the stars on the faint slope must be (on average) on the far (back) side. Therefore, one can select bright and faint samples of RCGs and examine their differences in the radial velocity and proper motion. The second effect we explore is based on the well-known fact that lensed bulge stars lie preferentially on the far side of the Galactic bar due to the enhanced lensing probability by the stars on the near side. This leads to several observable effects. For example, the lensed RCGs should be fainter compared with all observed red clump stars in the field (Stanek 1995; see also Zhao 1999a, 1999b, 2000 for other effects such as extinction and reddening for microlensing events toward the Large Magellanic Cloud). We will examine systematic differences in the proper motions and radial velocities of the lensed RCGs relative to all observed RCGs in the Galactic bar; a similar bias in the radial velocity for lensing events toward the Large Magellanic Cloud has been discussed by Zhao (1999b).

As this paper is the first feasibility study, we do not attempt to construct a detailed (or even self-consistent) model of the Galactic bulge. Our aim is to provide an order-of-magnitude estimate of the kinematic biases in the hope of motivating observations to be carried out, which may in turn provide strong constraints on the the model of the inner Galaxy and incentives for their refinement. The structure of the paper is as follows. In §2, we outline our model, and in §3 we present our main results. We discuss observational issues to detect these effects in §4. For definiteness, we shall restrict ourselves to studying the red clump stars in Baade's window ($l = 1^\circ$, $b = -3.9^\circ$).

2 MODEL

To explore both effects that we discussed above for RCGs, we need to adopt a bulge model, which is rather uncertain; there are a number of published analytical and numerical models of various complexities (see Han & Gould 1995 for a large selection of analytical models; see Zhao et al. 1996, Häfner et al. 2000, Fux 2001 and references therein for numerical models).

For illustrative purposes, we will take two simple analytical models in the literature for the Galactic bulge.

The first toy model we adopt is identical to the one used by Kiraga & Paczyński (1994). The bulge mass density distribution is approximated as axis-symmetric and is based on the study of Kent (1992). Note that there is no bar in this simple model. The bulge velocity distribution is assumed to be isotropic. Each of the three velocity components follows a Gaussian distribution with a dispersion of 100 km s^{-1} . In addition, the bulge stars on the near side rotate with a velocity of $+100 \text{ km s}^{-1}$ (in the same direction as the solar rotation) while those on the far side rotate in the opposite sense (see Kiraga & Paczyński for details). In this model, the streaming motion is purely tangential. The second model we consider is somewhat more realistic. It is based on the E2 bar model of Dwek et al. (1995). For the following discussions, it is convenient to establish a coordinate system centred on the bar with x , y and z corresponding to the major, intermediate and minor axes. The minor axis coincides with the vertical direction while the major axis has a viewing angle of $\theta_{\text{bar}} = 24^\circ$ from the line of sight (for an illustration of the bar geometry, see Figs. 6 and 11 in Stanek et al. 1997). The axial ratios are taken to be $1 : 0.42 : 0.28$. The luminosity-weighted velocity dispersions can be derived using the virial theorem (Belokurov & Evans 2001) as $\sigma_x = 100 \text{ km s}^{-1}$, $\sigma_y = 80 \text{ km s}^{-1}$ and $\sigma_z = 68 \text{ km s}^{-1}$, respectively. In addition, the stars on the near side have a streaming motion of $+50 \text{ km s}^{-1}$ parallel to the major axis, while the stars on the far sides move in the opposite sense. Note that the (rotational) sense of the streaming motion is similar to that adopted by Kiraga & Paczyński (1994), but a factor of two smaller in value.

The intrinsic luminosity function of red clump stars is assumed to follow a Gaussian distribution with a width $\sigma_0 \approx 0.2 \text{ mag}$ (Stanek et al. 1997); there is presumably no difference in the luminosity function for RCGs on the near and far sides. We assume that RCGs follow the same bulge mass distribution over a distance range from $D_{\min} < D_s < D_{\max}$; we take $D_{\min} = 0.5R_0$ and $D_{\max} = 1.5R_0$, where $R_0 = 8 \text{ kpc}$ is the distance to the Galactic centre. Other choices of D_{\min} and D_{\max} only change our results slightly. Note that the effect of extinction and reddening can be minimised by using the extinction-insensitive Wesenheit index, W_{V-I} (written as V_{V-I} in Paczyński et al. 1994).

RCGs are usually selected in the colour-magnitude diagram by requiring their colours and magnitudes to be in a certain range (e.g., Fig. 1 in Paczyński & Stanek 1998). Many red giants occupy the same region in the colour-magnitude diagram. As the luminosities of

red giants span a broad range they can be at either on the far side or on the near side at any given (apparent) magnitude. Therefore, they dilute the kinematic differences between a bright RCG sample and a faint one as their apparent brightness can not be used as an approximate measure of distance. We model the number counts of red giants as a linear function of the apparent magnitude (see eq. 1 in Paczyński & Stanek 1998). According to the model, within one magnitude of the RCG peak, red giants contribute about 60% of the total number. Therefore, red giants substantially dilute the offset signals if they cannot be separated from the red clump stars; we return to this issue in the discussion.

For the offset in kinematics between lensed and all observed RCGs, we need to calculate the microlensing optical depth and event rate. We consider both bulge self-lensing and lensing by the disc. Therefore, we need to specify the disc mass distribution and kinematics. As the offsets in the radial velocity and proper motion depend only on the *ratio* of the lensing frequency for stars on the near side and those on the far side, they do not depend on the mass function as the mass cancels out in the ratio.

For the disc mass distribution, we adopt the familiar double exponential form (Bahcall 1986)

$$\rho(r, z) = \rho_{\odot} \exp \left(-\frac{r - R_0}{3.5 \text{ kpc}} - \frac{|z|}{0.325 \text{ kpc}} \right), \quad (1)$$

where (r, ϕ, z) are the usual cylindrical coordinates (in units of kpc), and ρ_{\odot} is the local disc density, for which we take a value of $0.06 M_{\odot} \text{ pc}^{-3}$. The velocity dispersions are taken to be $\sigma_r = 30 \text{ km s}^{-1}$, $\sigma_{\phi} = 20 \text{ km s}^{-1}$, and $\sigma_z = 20 \text{ km s}^{-1}$, which are typical values in all disc models (e.g., Belokurov & Evans 2002). The disc lenses have a systematic rotation of $v_{\phi} = +220 \text{ km s}^{-1}$ at all distances. In addition, we also account for the solar motion relative to the local standard of rest (see e.g., Binney & Merrifield 1998).

Obviously, the optical depth and event rate need to be weighted properly by the source distance (see eqs. 5 and 11 in Kiraga & Paczyński 1994). For the lensing of RCGs, we assume that they are bright enough to be seen with equal probability at all distances (corresponding to $\beta = 0$ in the formalism of Kiraga & Paczyński 1994).

3 RESULTS

Monte Carlo simulations are performed to obtain our results; this is the easiest way to incorporate different source populations and selection strategies. In the following, we first discuss the offset in the radial velocity, V_r , and in the longitudinal proper motion, μ_l , between

the faint and bright samples of RCGs, and then discuss the offsets between the lensed and all observed RCGs.

3.1 Offsets in V_r and μ_l Between Faint and Bright Sub-samples of RCGs

As we discussed previously, the observed luminosity function of RCGs has a well defined peak in their number counts (see Fig. 5 in Stanek et al. 1997). The RCGs on the brighter side of the peak are (on average) on the front side of the bar and vice versa. We experimented with different ways of selecting ‘bright’ and ‘faint’ samples in order to maximise their differences in the radial velocity and proper motion. We found that the optimum ‘bright’ sample is formed by stars that are brighter than the peak magnitude by 0.2 to 0.4 magnitude. Similarly, the optimum ‘faint’ sample is formed by stars fainter than the peak magnitude by 0.2 to 0.4 magnitude. Notice that each sample also includes a background of red giant stars.

The shift in the radial velocity between the faint and bright samples depends on the model. In the Kiraga & Paczyński model, there is no radial streaming of stars, hence there is no shift in the radial velocity as the stars on the near and far sides have the same random kinematics. This is different for the Dwek et al. model, where we have streaming motions of $\pm 50 \text{ km s}^{-1}$ mostly along the radial direction as the bar is (by assumption) only 24° from the line of sight.

The left panel in Fig. 1 shows the distributions of radial velocity for the bright (dashed) and faint (solid) samples, respectively. Both distributions are roughly Gaussian with a dispersion of $\approx 110 \text{ km s}^{-1}$. The faint sample is shifted toward more negative radial velocities, with an average shift of $\approx 33 \text{ km s}^{-1}$. This shift can be understood qualitatively. The stars on the near side have an average radial velocity $(-10 + 50 \cos \theta_{\text{bar}}) \text{ km s}^{-1}$, where -10 km s^{-1} arises due to the solar motion ($+10 \text{ km s}^{-1}$) relative to the local standard of rest. Analogously, stars in the faint sample are mostly on the far side, and they have an average radial velocity $(-10 - 50 \cos \theta_{\text{bar}}) \text{ km s}^{-1}$. As the faint sample includes more stars on the far side, hence their radial velocities are more negative. The average shift between the bright and faint samples is about one third of the velocity dispersion along the line of sight ($\sim 100 \text{ km s}^{-1}$). We return to the feasibility of observing this shift in the discussion.

As the streaming motion we considered is in the plane of the Galaxy, we do not expect any shift in the latitudinal proper motion, so we will only consider the shift in the longitudinal direction, μ_l . The shift in μ_l between the bright and faint samples again depends on the

model. In the second model, the streaming motion is mostly radial, so the proper motion shift is relatively small. However, for the Kiraga & Paczyński model, there is a tangential streaming motion of $+100 \text{ km s}^{-1}$ for stars on the near side and -100 km s^{-1} on the far side, and so the offset becomes more apparent. The left panel in Fig. 2 shows the distributions of proper motion for the bright (dashed) and faint (solid) samples, respectively. The proper motions for the faint sample is shifted toward a more negative value, by an average amount of 1.6 mas yr^{-1} ; the dispersion for the faint sample is also about 10% smaller. To understand these trends, let us recall that for a star with velocity v_l (in units of km s^{-1}) and at distance D_s (in units of kpc) has a proper motion of $\mu_l \approx 0.2v_l/D_s \text{ mas yr}^{-1}$. In the *heliocentric* frame, stars on the far side move with a streaming motion of $v_l = -300 \text{ km s}^{-1}$ while stars on the near side move with $v_l = -100 \text{ km s}^{-1}$. As the faint sample includes more stars from the far side, their proper motions are therefore more negative relative to the bright sample. The average shift is roughly proportional to the value of the tangential streaming motion; it is about one half of the dispersion in the proper motion of approximately 3 mas yr^{-1} for all observed stars. The dispersion of the faint sample is smaller because $\mu_l \propto D_s^{-1}$ and faint RCGs are on average at slightly larger distances.

3.2 Offsets in V_r and μ_l Between Lensed and All Observed RCGs

The shift in the radial velocity between the lensed and all observed RCGs depends on the models. In the first model where there is no radial streaming of stars, there is no shift in the radial velocity as the stars on the near and far sides have the same random kinematics. This is different for the second model, where we do have radial streaming motions.

The right panel in Fig. 1 shows the distributions of radial velocity for the lensed (solid) and all observed (dashed) RCGs, respectively. The curve predicted for all observed stars has a negative mean value around -10 km s^{-1} partly due to the solar motion with respect to the local standard of rest. However, in this model, the stars on the far side move with $-50 \cos \theta_{\text{bar}} \text{ km s}^{-1}$ along the line of sight and those on the near side move in the opposite direction. As the optical depth and lensing event rate are higher for stars on the far side, radial velocities of the lensed sources are shifted toward more negative values. The difference in the average radial velocity is about $\sim 10 \text{ km s}^{-1}$. This is smaller than the offset between the bright and faint samples that we discussed in §3.1. We found that this shift is roughly

proportional to the value of the radial streaming motion. In any case, the average shift is fairly small compared with the velocity dispersion along the line of sight ($\sim 100 \text{ km s}^{-1}$).

The shift in the proper motion between the lensed and all observed RCGs again depends on the model. In the second model, the streaming motion is mostly radial, so the shift in proper motion is relatively small. However, for the first model, where there is a tangential streaming motion of $+100 \text{ km s}^{-1}$ for stars on the near side and -100 km s^{-1} on the far side, the offset becomes noticeable. The right panel in Fig. 2 shows the distributions of proper motion for the lensed stars (solid) and all observed stars (dashed), respectively. The curve for the overall population has an average proper motion of $\approx -5.8 \text{ mas yr}^{-1}$ due to the solar motion around the Galactic centre. The curve for the lensed population is shifted toward more negative proper motions. This is because stars on the far side move opposite to the solar rotation, and as they have larger optical depths and are more frequently lensed, their proper motions are shifted toward more negative longitudinal values. The average shift in the proper motion is about 1.2 mas yr^{-1} , which is smaller than its dispersion, about 3 mas yr^{-1} . As expected, this offset is roughly proportional to the value of the tangential streaming motion.

4 DISCUSSION

In this paper we have studied how to use red clump giants (RCGs) to constrain the kinematics of stars in the Galactic bar. The basic idea is that stars on the near and far sides may have different streaming motions, and if we can select two samples with one preferentially on the near side and the other on the far side, then they should show differences in the radial and tangential streaming motions. We have examined two ways that we can select such samples. The first method selects a bright sample and a faint one with the peak magnitude of the number counts of RCGs as the approximate dividing line. The RCGs in the faint sample is (on average) more on the far side of the bar and vice versa. The second method relies on the fact that stars on the far side are preferentially microlensed due to the enhanced lensing probability by the stars on the near side and in the disc. Hence the lensed stars and all observed stars should behave differently in kinematics.

We illustrate the kinematical differences in the context of two simple models of the Galactic bulge. In the first (axis-symmetric) model, the streaming motion is purely tangential, while in the second (more realistic) bar model the streaming motion is more or less

radial. In reality, the streaming motions in the Galactic bar may have both a radial component and a tangential one, so our numbers should be taken as rough order-of-magnitude estimates.

We found that the difference in the radial velocity between the bright and faint samples can reach $\delta V_r \approx 33 \text{ km s}^{-1}$ for a radial streaming motion of 50 km s^{-1} . The difference is substantially reduced by the population of red giants that occupy the same part of the colour-magnitude diagram as the RCGs, as they have a large span in luminosity, so a brighter magnitude does not signal that a star is closer to us on average. If there is an effective way of differentiating red giants and red clump stars, then the differences in the radial velocity and proper motion can be much larger. This can be, for example, done by examining colours as RCGs occupy a slightly bluer part of the colour-magnitude diagram. Spectroscopic observations may also ultimately provide features that distinguish red giants and RCGs. For example, if the contribution of red giants can be reduced by one half, then the shift in the proper motions can be as high as 2.3 mas yr^{-1} , while that for the radial velocity can reach 50 km s^{-1} . In comparison, we find that the shift between the lensed stars and overall population of stars is more modest, about 10 km s^{-1} for a radial streaming motion of 50 km s^{-1} .

The velocity dispersion along the line of sight is about $\sigma \approx 100 \text{ km s}^{-1}$, so in order to see this shift at the 2σ level, from Poisson statistics, we only need to obtain the radial velocity for about $(2 \times \sigma / \delta V_r)^2 \approx 100$ stars even for $\delta V_r = 20 \text{ km s}^{-1}$. The required number is moderate, but is within reach of multi-object spectrographs available on many large telescopes. For example, the FORS1 instrument on VLT has 19 slits that can be efficiently used to derive the radial velocities of lensed stars and field stars simultaneously. Other instruments such as 2dF² which can take up to 400 spectra simultaneously should also be explored. We note that for RCGs, blending is not a severe problem as they are so bright, so their radial velocities can be measured without much difficulty. In any case, we only require an accuracy of $\sim 10 - 20 \text{ km s}^{-1}$ per star, since the dispersion in the radial velocity for the bulge stars is of the order of 100 km s^{-1} .

For the shift in the proper motions, we find that a value of 1.6 mas yr^{-1} between the bright and faint samples of RCGs for a tangential streaming motion $\overline{V}_l = 100 \text{ km s}^{-1}$. The shift scales roughly linearly with \overline{V}_l . The difference is about 1 mas yr^{-1} between the lensed

² <http://www.aoa.gov.au/2df/>

and overall population of bright stars. These shifts are not much smaller than the dispersion in the proper motion, approximately 3 mas yr^{-1} . The shifts can be detected with HST or even ground-based instruments. To do this, only a modest number of RCGs need to be monitored to measure the relative shifts in proper motions. The relative proper motion may be feasible to detect even from the ground. Soszyński et al. (2002) demonstrated that proper motions as small as 4 mas yr^{-1} can be measured with OGLE II data. This accuracy is achieved through a combination of the new difference image analysis software (Eyer & Woźniak 2001) and a large number of data points for any given star, which reduces the astrometric error through Poisson statistics. The camera system of OGLE III yields much better images than that of OGLE II as the latter operates in the drift scan mode and produced somewhat worse point spread functions. Therefore it seems possible (although still to be demonstrated) that proper motions of many red clump stars, including lensed ones, can be obtained using data from microlensing surveys (e.g., OGLE III), requiring no extra observing resources.

In this paper we have only explored the shifts in the radial velocity and proper motion in Baade's window. Clearly there must be a spatial dependence of these shifts. The OGLE III collaboration is currently monitoring many fields around the Galactic centre, covering from -7° to 6° in latitude and -12° to 12° in longitude³. Red clump stars and microlensing events will become available over large areas, and so it will be very interesting to detect the spatial variation of the shifts in the radial velocity and proper motion. Such observations will likely provide strong constraints on the Galactic bar parameters, and stimulate further theoretical efforts to build a better and self-consistent model of the inner Galaxy. Finally, we point out that if future astrometric missions, SIM and GAIA⁴, perform as planned, they will directly measure the radial depth of the galactic bar by determining parallax's for a number of stars. This will make our suggestion obsolete, but not sooner than in a decade.

We thank Martin Smith, David Spergel, and Hongsheng Zhao for helpful discussions. S.M. acknowledges travel support by Princeton University. This project was supported by the NSF grant AST-1206213, and the NASA grant NAG5-12212 and funds for proposal #09518 provided by NASA through a grant from the Space Telescope Science Institute, which is operated by the Association of Universities for Research in Astronomy, Inc., under NASA contract NAS5-26555.

³ For detailed field coordinates, see <http://www.astrowu.edu.pl/~ogle/ogle3/ews/gb-ews.jpg>

⁴ <http://sim.jpl.nasa.gov>; <http://astro.estec.esa.nl/GAIA/>

REFERENCES

Alard C., Guibert J. (DUO), 1997, 326, 1

Alcock C. et al. (MACHO), 1993, *Nature*, 365, 621

Alcock C. et al. (MACHO), 2000, *ApJ*, 541, 734

Aubourg E., et al. (EROS), 1993, *Nature*, 365, 623

Bahcall J. N., 1986, *ARA&A*, 24, 577

Belokurov V., Evans W.N., 2002, *MNRAS*, in press (astro-ph/0202042)

Binney J., Merrifield M., 1998, *Galactic Astronomy*, p. 628 (Princeton: Princeton University Press)

Blitz L., Spergel D.N.S., 1991, *ApJ*, 379, 631

Bond I. A. et al. (MOA), 2001, *MNRAS*, 327, 868

de Vaucouleurs G., 1964, in *IAU Symp. 20, The Galaxy and the Magellanic Clouds*, ed. F. J. Kerr & A. W. Rodgers (Canberra: Australian Acad. Sci.), p. 195

Derue F. et al. (EROS), 2001, *A&A*, 373, 123

Evans W.N., Belokurov V., 2002, *ApJ*, 567, L119

Eyer L., Woźniak P.R., 2001, *MNRAS*, 327, 601

Fux R., 2001, *A&A*, 373, 511

Gould A., 1996, *PASP*, 108, 465

Häfner R., Evans W.N., Dehnen W., Binney J., 2000, *MNRAS*, 314, 433

Han C., Gould A., 1995, *ApJ*, 447, 53

Han C., Gould A., 1996, *ApJ*, 467, 540

Kiraga, M., Paczyński, B., 1994, *ApJ*, 430, L101

Paczyński B. et al. (OGLE), 1994, *AJ*, 107, 2060

Paczyński B., 1986, *ApJ*, 304, 1

Paczyński B., 1996, *ARA&A*, 34, 419

Paczyński B., Stanek, K. S., 1998, *ApJ*, 494, L219

Soszyński I. et al. (OGLE), 2002, astro-ph/0205289

Stanek K.Z., 1995, *ApJ*, 441, L29

Stanek K.Z. et al. (OGLE), 1994, *ApJ*, 429, L73

Stanek K.Z. et al. (OGLE), 1997, *ApJ*, 477, 163

Stanek K. Z., Kaluzny J., Wysocka A., Thompson I., 2000, *AcA*, 50, 191

Udalski A. et al. (OGLE), 1993, *AcA*, 43, 289

Zhao H.S., 1999a, ApJ, 527, 167

Zhao H.S., 1999b, ApJ, 526, 141

Zhao H.S., 2000, ApJ, 530, 299

Zhao H.S., Rich, R. M., Spergel, D. N, 1996, MNRAS, 282, 175

Zoccali M., et al. 2000, AJ, 530, 418

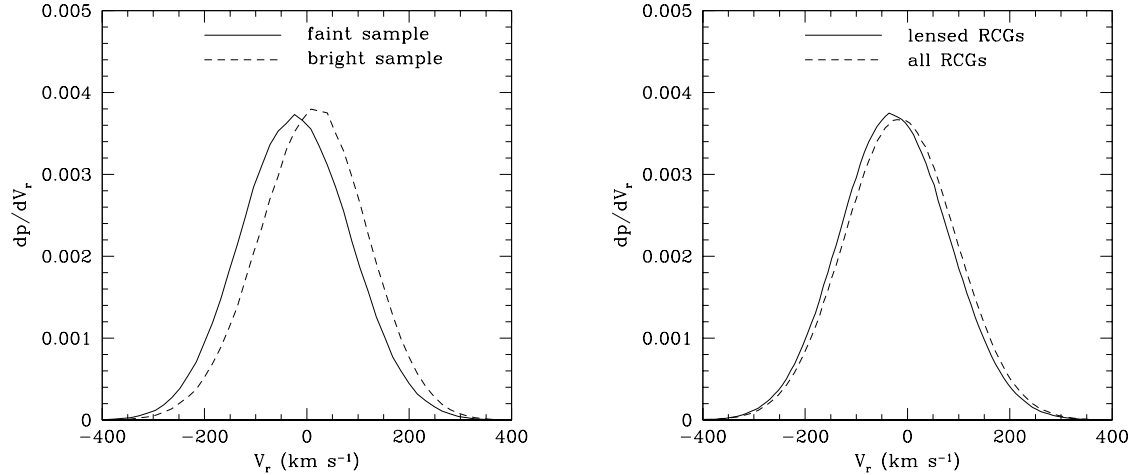


Figure 1. Normalised differential probability distributions of radial velocities. For the *left* panel, the solid (dashed) line shows the distribution for stars fainter (brighter) by 0.2 to 0.4 magnitude than the magnitude where the number counts of red clump giants (RCGs) peak. The average shift between these two populations is about 33 km s $^{-1}$. The *right* panel shows the distributions for lensed (solid) and all observed (dashed) stars, respectively. The average shift between these two populations is about 10 km s $^{-1}$. In both panels, the Galactic bulge is modelled as a bar with the major axis 24° away from the line of sight. The bulge sources have streaming motions parallel to the major axis: stars on the near side move with +50 km s $^{-1}$ in the same sense of Galactic rotation while stars on the far side move in the opposite sense.

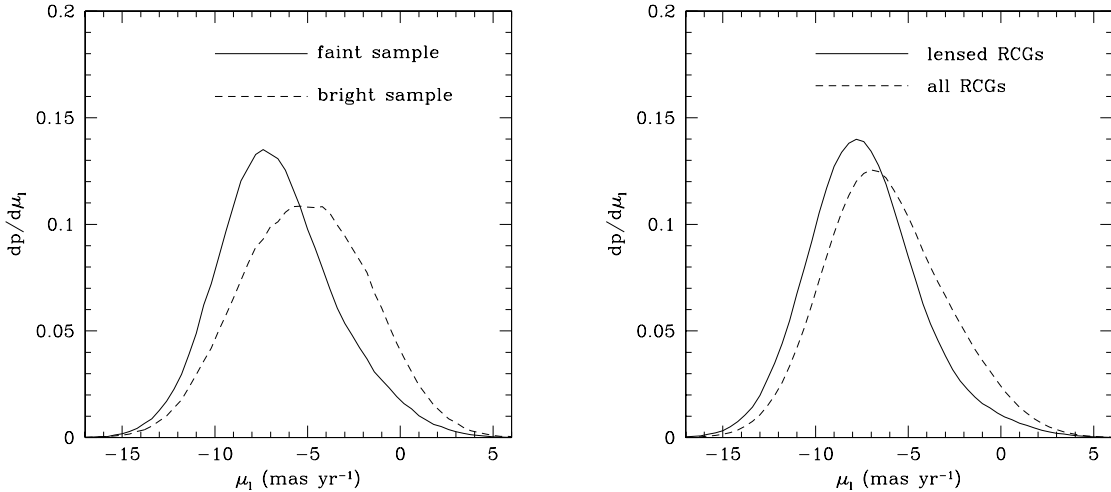


Figure 2. Normalised differential probability distributions of proper motions in the longitudinal direction in the Kiraga & Paczyński (1994) model. For the *left* panel, the solid (dashed) line shows the distribution for stars fainter (brighter) by 0.2 to 0.4 magnitude than the magnitude where the number counts of red clump giants peak. On average, the fainter population is shifted to a more negative proper motion by about 1.6 mas yr $^{-1}$. For the *right* panel, the distributions for lensed and all observed RCGs are shown as the solid and dashed lines, respectively. The lensed population is shifted to a more negative proper motion of about 1.2 mas yr $^{-1}$ on average. For both panels, the bulge sources are assumed to have a constant streaming motion perpendicular to the line of sight of 100 km s $^{-1}$ but with opposite signs on the near and far sides of the Galactic centre.